Thin Solid Films 763 (2022) 139563

Contents lists available at ScienceDirect

Thin Solid Films

journal homepage: www.elsevier.com/locate/tsf

Detection and analysis of phage M13KO7 using biosensor based on imaging ellipsometry

Cai Qi [a,*], Yanxu Zhang [a], Wenjing Lei [a], Gang Jin [b,c,d]

[a] Henan–Macquarie University Joint Centre for Biomedical Innovation, School of Life Sciences, Henan University, Jinming Avenue, Kaifeng, Henan, 475004, China
[b] NML, Institute of Mechanics, Chinese Academy of Sciences, #15, Beisihuan West Rd., Beijing, 100190, China
[c] School of Fundamental Physics and Mathematical Sciences, Hangzhou Institute for Advanced Study, University of Chinese Academy of Sciences, #1, Sub–Lane Xiangshan, Hangzhou, Zhejiang, 310024, China
[d] School of Engineering Sciences, University of Chinese Academy of Sciences, #19, Yu–Quan Road, Beijing, 100049, China

ARTICLE INFO

Keywords:
Optical biosensor
Imaging ellipsometry
Microfluidic system
Phage M13KO7
Detection

ABSTRACT

Antibody GP8 (anti-GP8) was used as a ligand to detect phage M13KO7 using a biosensor based on imaging ellipsometry (IE) without oriented ligand immobilization. When the phage M13KO7 in a sample interacted with the antibody in a microarray, a complex formed upon their affinity, and the layer covering the surface cell of the interaction became thicker. The variation in layer thickness was represented by gray-scale (or brightness) variation of the IE image. Direct and oriented immobilization of the antibody were analyzed to identify the best binding locations to capture the phage. In direct immobilization, the phage could be captured by anti-GP8 and not antibody GP3 (anti-GP3), which was attributed to different copy numbers of the coat proteins on the body of the phage specific to the two antibodies. This indicated that different binding locations could produce different detection efficiency. In oriented immobilization, the phage could be captured by the protein G–Fc-anti-GP3 model, with a low detection efficiency. In contrast, the avidin–biotin-based oriented immobilization could capture the phage with a high detection efficiency. Specifically, it could expose more Fab domains of anti-GP3 labeled with biotin; one avidin had four biotin-binding sites. To confirm detection and analyze binding location, the phage M13KO7 was imaged by transmission electron microscopy and atomic force microscopy. Our results suggest that binding location plays a significant role in the detection of big targets and contributes to enhancing biosensor detection sensitivity.

1. Introduction

Binding forces between biomolecules are crucial in most biological processes [1]. In the development of biosensors, analyzing binding forces between ligands and target molecules is important to evaluate detection efficiency and sensitivity [2, 3]. Different binding locations on a target molecule directly affect the binding force. Ligand immobilization and different biomolecules utilized as ligands are closely related to binding location. Immobilizing a ligand usually involves direct attachment to the substrate without surface modification and covalent immobilization with surface modification [4]. Covalent immobilization includes random and oriented immobilization. When biomolecules are randomly immobilized with direct attachment, the ligands can suffer partial denaturation and tend to leach or wash off the surface. They can also be competitively adsorbed by other biomolecules with a higher activity [5]. This indicates that immobilization through direct attachment is not firm because of posture and low strength. Covalent immobilization has been demonstrated as the preferred method of attaching proteins to a silicon surface due to a strong and stable linkage [6]. Oriented immobilization maintains the orientation or posture of ligands to expose their target interacting domains. Specific molecules have been used to link surfaces to ligands, such as protein A [7]. Binding affinity and kinetics as well as force magnitude between ligands and target molecules have been studied [8–14]. The interaction force between human immunoglobulin G (H-IgG) and goat anti-human IgG is approximately 342 piconewtons (pN) [15]. It was shown that a pair of molecules could be pulled away from one another by a small sphere as a moment of force. If the small sphere was regarded as a big target, the big target was not easily captured owing to insufficient force. However, suitable force action points or binding locations for capturing big targets

* Corresponding author.
E-mail address: qicaisucceed@henu.edu.cn (C. Qi).

https://doi.org/10.1016/j.tsf.2022.139563
Received 9 June 2022; Received in revised form 24 October 2022; Accepted 25 October 2022
Available online 27 October 2022

have been hardly addressed in previous studies.

Ellipsometry is a powerful method for determining both the optical constants and thickness of thin films, and it has been used in scientific labs and industrial companies [16]. Biosensors based on imaging ellipsometry (BIE) have been applied mainly in biomedical fields, such as in 1) bacterium detection [17–19], 2) biomolecule interaction [20, 21], 3) cell factor and its receptor interaction [22], 4) cancer markers testing [23], 5) hepatitis B detection [24], 6) chloramphenicol detection in real milk samples [25], and 7) procalcitonin detection [26]. It is necessary to analyze certain factors regarding the force of capturing targets with practical examples for further development of BIE.

In this study, we used antibody GP8 (anti-GP8) to detect phage M13KO7 without oriented antibody immobilization. We checked direct and oriented immobilization of antibody against phage M13KO7 (anti-M13) using BIE to analyze suitable binding locations between the antibody and the phage. Antibody GP3 (anti-GP3) and anti-GP8 were immobilized as ligands directly on the surface. To perform oriented ligand immobilization, the protein G–Fc-anti-GP3 and avidin–biotin-oriented immobilization models were used. Moreover, the phages M13KO7 were characterized at a microscopic level by a transmission electron microscope (TEM) and atomic force microscope (AFM). We analyzed factors influencing the capacity of binding locations to capture phages M13KO7 and illustrated this issue with intuitive schemes.

2. Experimental details

2.1. Biosensor substrate, chemicals, biological reagents, and phage samples

Silicon wafers were purchased from Luoyang Monocrystalline Silicon Factory, Henan, China; 3-aminopropyltriethoxy-silane (APTES, 99% v/v) from ACROS; and H_2O_2 (30%), H_2SO_4 (98%), and absolute ethanol from Beijing Bei Hua Fine Chemicals Co., Ltd. Glutaraldehyde (50% aqueous solution, photographic), avidin, H-IgG, bovine serum albumin (BSA) and Tween 20 were purchased from Sigma. All chemicals were of analytical grade. Anti-GP3 and anti-GP3 labeled with biotin (bio-anti-GP3) were purchased from Exalpha Biologicals; these antibodies can specifically identify minor coat protein pIII (protein GP3) on the head of the phage M13KO7 [27]. Natural and purified phage M13KO7 (5×10^{11} pfu/mL) samples and anti-GP8 were provided by the Institute of Biophysics, Chinese Academy of Sciences; this antibody can specifically identify major coat protein pVIII (protein GP8) on the body of the phage M13KO7 [28]. Phosphate-buffered saline (PBS, 140 mM NaCl, 2.7 mM KCl, 10 mM Na_2HPO_4, 1.8 mM KH_2PO_4, pH 7.3) and PBST (PBS with 1% Tween 20) were prepared in deionized water (Millipore, Bedford, MA. Resistivity 18.2 MΩcm at 25°C; Total Organic Carbon ≤5 ppb; Particles is < 1 p/mL; Bacteria < 1 cfu/mL; Pyrogen < 0.001 EU/mL; Rnases < 0.01 ng/mL; Dnases < 4 pg/mL; Flow Velocity: four flow rates are available with a maximum of 2 L/min.). Resistivity (R) is one of the important parameter of deionized water. R = 1/X. X = FΣ CiZiUi, X is conductivity; F is faraday constant; Ci is ion concentration; Zi is charge number of ions; Ui is ionic mobility. Theoretically, the conductivity of completely ion free ultrapure water is 0.055 μS/cm at 25 °C, so the resistivity is approximately 18.2 MΩcm at 25°C. All samples were diluted with PBST. AFM experiments were performed by the Institute of Chemistry, Chinese Academy of Sciences. TEM experiments were performed by the Institute of Biophysics, Chinese Academy of Sciences. The ultrasonic machine was produced by Jiangsu Kunshan Ultrasonic Instruments Co., Ltd., China.

2.2. BIE

BIE has been developed in our laboratory for the purpose of performing parallel immunoassays. This technique is based on the combination of an integrated microfluidic reactor array system and imaging ellipsometry (IE). It can be performed as a label-free technique. Using a silicon wafer as substrate modified with APTES and glutaraldehyde, an antibody (or antigen) can be covalently bound to different cells on the surface of the silicon wafer due to a reaction of the Schiff base with –CHO, based on the microfluidic model for a microarray. In this case, each cell of the microarray may function as an immunological probe, which can capture corresponding antigens (or antibodies) in the solution. When the corresponding antibodies (or antigens) in the solution interact with the immunological probe in a microarray, they form a complex upon their affinity and the layer covering the surface cell of the interaction becomes thicker (or surface concentration increases). A significant increase in the attached layer thickness (or surface concentration) indicates that the solution contains the antibody (or antigen). IE is used to detect a protein layer pattern on a microarray surface. Distribution of the lateral thickness (or surface concentration) in the protein layer pattern is simultaneously detected, which may further point to the existence of antibodies in the tested solution.

IE is a technique for displaying characteristics of ultra-thin films and surfaces [29–32]. The ellipsometry signal is measured by null ellipsometry which is based on an instrument where the polarizing elements (polarizer and analyzer) are rotated until the signal at the detector is zero (null). The optical parameters can then be deduced from the angular positions of the polarizer and analyzer. For IE, which is used to detect a large-area sample with lateral distribution in layer thickness, null ellipsometry could not be carried out over the entire surface simultaneously due to the fact that different areas will yield different polarization changes. A possible solution is to use off-null mode in an ordinary null ellipsometer. The optical components in the system are adjusted to fulfill the null conditions on a silicon wafer without adsorbed layers, and the off-null ellipsometric principle is used to measure the adsorption layer thickness [30]. The incident wave of polarized light irradiates the sample as a probe beam and is thereby modified, which makes the reflected or transmitted beam carry sample information, such as protein layer thickness. The reflected intensity detecting using IE is represented by gray-scale. Variation in layer thickness was represented in gray-scale variation in the IE image. When the refractive index is invariant, the gray-scale value is directly proportional to the square of the protein layer thickness in the range of 0–30 nm layer thickness, i.e. $I = kd^2$, where I is the light intensity and d is the layer thickness. Under the same conditions in terms of protein and ellipsometry apparatus, k is constant and can be determined from a protein layer with known gray-scale value and thickness of thin films [29]. Moreover, there is a relationship between surface concentration and film thickness: surface concentration ($\mu g/cm^2$) ≈ K × d, where K = 0.12 [32]. Thus, the gray-scale value reflects directly the layer thickness or the surface concentration. The higher the gray-scale value, the thicker the layer and the higher the surface concentration.

2.3. Detection procedure of phage M13KO7 using BIE

The detection procedure was similar to that of previous studies [19]. First, silicon wafers were chosen as the substrate, then modified with chemical reagents to form chemical groups on their surface to covalently immobilize proteins as ligands. The aldehyde group, $-(CH_2)_3N{=}CH(CH_2)_3\text{-}CHO$, was produced on the silicon wafer surface using this surface modification method reported in a previous study [6]. Second, a microfluidic system was used to add the reagents and samples [24]. The modified wafer was placed in the microfluidic system so that its surface was patterned to form regular small cells. In direct immobilization, anti-M13 was directly added as a ligand and immobilized to form a sensing surface. In oriented immobilization, several guiding and specific molecules were added as oriented molecules and immobilized before ligand immobilization. Then, anti-M13 was directionally immobilized as a ligand on the surface of these oriented molecules. Finally, phage samples were added to the sensing surface. If the samples contained phage M13KO7, the phage were specifically captured by the sensing surface, resulting in layer thickness variation. Subsequently, the wafer

was rinsed with deionized water and taken out of the system. After rinsing 2-3 times with plenty of deionized water and drying under nitrogen, the microarray pattern was detected and recorded as images in gray-scale using IE. The quantity of phages captured by anti-M13 was directly proportional to the gray-scale value within the range of 0–30 nm layer thickness. High gray-scale values of microarray cells represented greater force or a more appropriate binding location.

2.4. Direct immobilization of anti-GP3 and anti-GP8

When a modified wafer was placed on the micro-reaction interface of the microfluidic system, its surface was patterned to form regular small cells (physical dimensions volume of a cell: length × width × depth is $1.5 \times 1 \times 0.1$ mm^3, and the square area was observed in the IE image). The anti-GP3 without a biotin label was added to the microfluidic system according to the designed surface arrangement style using a procedure (0.1 mg/mL, 10 μL/cell, passing the surface at 2 μL/min). The anti-GP3 could be covalently immobilized on the modified substrate. The cells were rinsed with PBST, and each cell was then blocked with BSA for 40 min using a procedure (10 mg/mL, 40 μL/cell, passing the surface at 1 μL/min). Anti-GP8 was immobilized directly on another modified silicon wafer using the same procedure as anti-GP3.

2.5. Categories of oriented immobilization of anti-GP3

2.5.1. Oriented immobilization of anti-GP3 using protein G

Protein G was added to cells simultaneously using a procedure (0.25 mg/mL, 10 μL/cell, passing the surface at 2 μL/min) optimized according to the design for the surface arrangement style. Then, protein G was covalently immobilized on the modified substrate. Briefly, the cells were rinsed with PBST, and each cell was then blocked with BSA before adding anti-GP3 (0.1 mg/mL, 10 μL/cell, passing the surface at 2 μL/min). Thus, oriented immobilization of anti-GP3 was achieved.

2.5.2. Oriented immobilization of anti-GP3 with the avidin–biotin model

Avidin was covalently immobilized on the modified substrate using a procedure (0.5 mg/mL, 10 μL/cell, passing the surface at 2 μL/min). The cells were rinsed with deionized water, and each cell was then blocked with BSA before adding bio-anti-GP3 (0.1 mg/mL, 10 μL/cell, passing the surface at 2 μL/min). Since bio-anti-GP3 on these cells could specifically identify minor coat protein GP3 on the head of phage M13KO7, some identical immunological probes of phage M13KO7 were formed, which were capable of detecting separate samples simultaneously. The interaction between biotin and avidin is one of the strongest protein–ligand interactions exhibiting high affinity and specificity [33].

2.6. Analysis with TEM and AFM

The shape, size, hardness, and structure of phages M13KO7 were identified using TEM and AFM, which were significant for analyzing the binding locations and the focus of capturing the phage. The cells of anti-M13 and phage on the silicon wafer were imaged with AFM in tapping mode, and different sizes and frequencies were used to provide more information about shape and size. An ultrasonic method was adopted to disperse the phage sample, and 0.5–10 μL sample was added on the gilder grids of TEM. TEM image of phage M13KO7 in liquid culture medium according to the scan model accelerating voltage 50.0 kV and range 300 nm. The TEM image was used to help find the phage on the silicon wafer or mica using AFM. The phage sample was added to the mica surface and scanned with AFM that provided the original configuration of phage M13KO7 as the control image. Finally, the phage detection cell on the silicon wafer was scanned with AFM. The corresponding cells on silicon wafer were marked with a marker pen before AFM observation. AFM height images in tapping mode of phage M13KO7 on the mica surface in (5.0 × 5.0 μm). AFM height images of phage M13KO7 on the mica surface in (1.0 × 1.0 μm) The whole image was scanned under 5 μm and 0.8846 Hz, and the top left image was scanned under 1.2 μm and 1.209 Hz. AFM image of scanning under 5 μm and 1.327 Hz for phage M13KO7 on the sensing surface formed by antibody.

3. Results and discussion

3.1. Detection of phage M13KO7 using direct immobilization of anti-GP3 and anti-GP8

Phage M13KO7 was detected using anti-GP3 as a ligand. As shown in Fig. 1A, the gray-scale value of the top four cells did not change when the phage sample (5×10^{11} pfu/mL in PBST, 10 μL/cell, passing the surface at 2 μL/min, incubation time of phage with antibody was 10 min) flowed through the anti-GP3 cells. This indicated that the phage could not be captured by the sensing surface. However, using anti-GP8 as the ligand, the gray-scale value of the top four cells increased significantly compared to that of the bottom two cells after adding PBST buffer (Fig. 1B). Phages M13KO7 were captured by anti-GP8, which resulted in an increase in surface concentration. This result was reproduced more than three times, indicating that direct immobilization of anti-GP8 could capture phages M13KO7.

3.2. Detection of phage M13KO7 using two kinds of oriented immobilization of anti-GP3

One kind of oriented immobilization was the interaction of protein G with the Fc fragment of anti-GP3, leaving the Fab regions available for binding to phage M13KO7 (Fig. 2A). The gray-scale variation of protein G and avidin immobilization on the surface was not evident, as shown by the lack of signals in the top row of Fig. 2. In contrast, the gray-scale variation of anti-GP3 or anti-GP8 immobilization is evident in the bottom two cells (Fig. 1). This finding is explained by the different molecular weights of these molecules. The molecular weight of the antibody (anti-GP3 or anti-GP8) is approximately 150 kDa, which is about three times larger than that of protein G and avidin (65–68 kDa). The gray-scale values of the bottom four cells with immobilized protein G and anti-GP3 are higher than those of the upper two cells with immobilized protein G only, indicating that protein G could bind anti-GP3. The bottom two cells among the four cells binding anti-GP3 were used to detect phage M13KO7. The gray-scale value of the two cells detected with phage M13KO7 was increased by approximately 29.7% (c1 and c2 in Fig. 2A) compared to that of the two control cells (b1 and b2 in Fig. 2A). This finding suggested that phage M13KO7 could be captured by the sensing surface of oriented immobilization of anti-GP3 through protein G with a low detection efficiency. When the oriented immobilization model of biotin and avidin was used to immobilize anti-GP3, the gray-scale value of two cells detected with phage M13KO7 increased by approximately 54.5% (f3 and f4 in Fig. 2B) compared to that of the two control cells (e3 and e4 in Fig. 2B). This increase is evident to the naked eye in the gray-scale image. Phage M13KO7 was captured effectively by the sensing surface of anti-GP3.

Oriented immobilized antibodies are more likely to capture their target. The oriented molecules such as protein G, or avidin, can adjust the orientation of ligands such that the functional domain is better displayed outside to improve the detection efficiency. Previously, we investigated the feasibility of using a silicon surface coated with protein A to immobilize antibodies as an alternative to direct immobilization [7]. Protein A can specifically bind to the Fc region of various mammal immunoglobulins, while leaving the Fab regions available for antigen binding [34, 35]. Protein G has the same function as protein A and can immobilize more antibody types than protein A. However, oriented immobilization using protein G captured phage M13KO7 with a low efficiency. This can be attributed to the insufficient force, owing to unsuitable binding locations, to capture the large M13KO7 target. The oriented immobilization model of biotin and avidin was used to

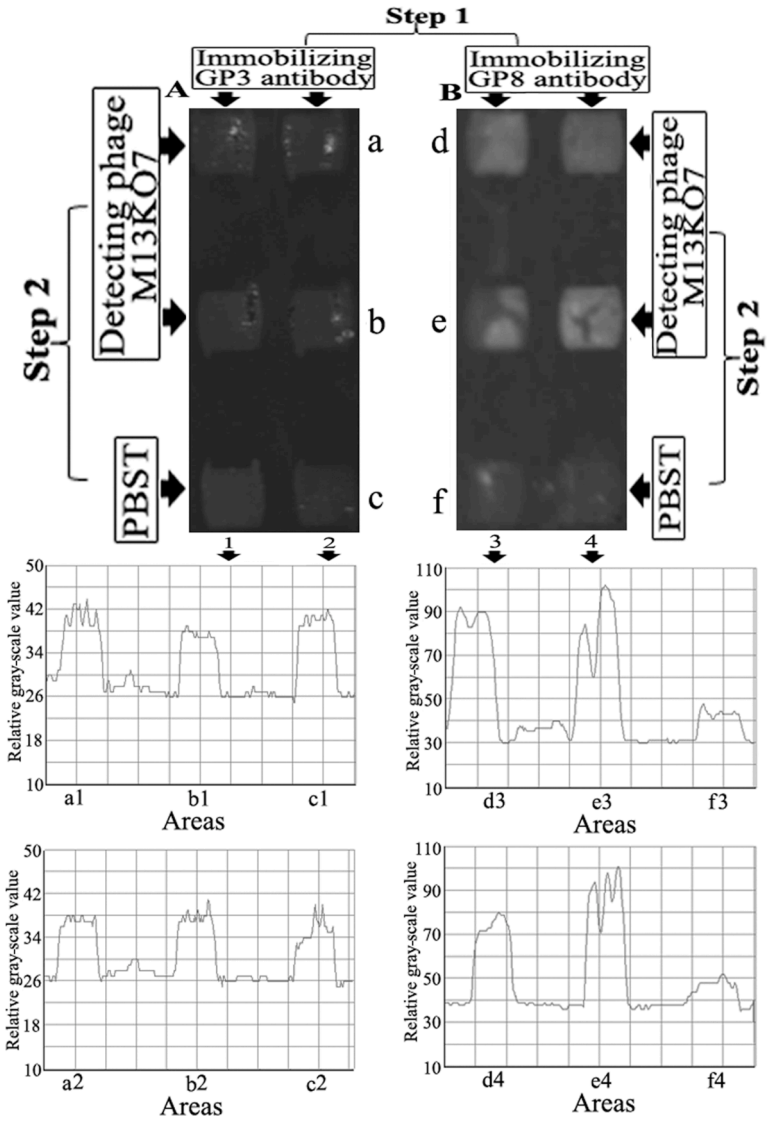

Fig. 1. Phage M13KO7 detection using anti-GP3 and anti-GP8 direct immobilization. (A) Anti-GP3 was used as a ligand to detect the phage M13KO7. (B) Anti-GP8 was used as a ligand to detect the phage M13KO7.

immobilize anti-GP3. The Fc part of anti-GP3 is lysine-rich, and biotin was labeled on anti-GP3 based on the covalent bonding between the carboxyl of biotin and ε amide of lysine [36, 37]. As a result, the Fab regions of anti-M13 were displayed away from the substrate, which facilitates their binding with the antigenic domain and hence an improved biosensor sensitivity. Thus, the oriented immobilization model of biotin and avidin is able to capture the phage M13KO7. The above findings in relation to protein G indicate that the phage was captured with a low efficiency by displaying only the antibody domain. This suggests that there must be other reasons for the capture of phage M13KO7. One reason might be that the affinity (10^{15} M^{-1}) between biotin and avidin was higher than that between antibody and antigen (10^{7}–10^{8} M^{-1}, which is similar to the affinity between protein A or G and antibody). Hence, the immobilized antibody was strongly bound to the surface such that it was prevented from being taken away by the phage. Another reason may be attributed to the structure of avidin. An avidin molecule has four biotin-binding sites and therefore can theoretically immobilize multiple biotin molecules labeled on antibodies. Moreover, multiple biotin labels might also be present on one antibody molecule. The more bonds or binding locations, the greater the binding force to capture the big target. This increases the chance and number of antibodies binding to phage. Therefore, the phage can be captured with a high efficiency by the oriented immobilization of biotin and avidin.

3.3. Analysis of shape and size of phage M13KO7 using TEM and AFM

The appearance and shape of the phage M13KO7 were determined by TEM and AFM (Fig. 3). Loose, long, and filamentous phages were seen under TEM in Fig. 3A, which was their original and overall configuration in liquid. Fig. 3B and C show the phage M13KO7 in different scales on the mica surface using AFM. The long filamentous phage with a tight structure lay flat on the mica surface, and its length, height and width were approximately 1.5 μm, 4.42 nm and 39.21 nm, respectively [38]. Furthermore, a large amount of filamentous phage was captured by bio-anti-GP3, which was consistent with previous reports, including AFM images of an anti-fd/anti-CPV/anti-CB3 ViriChip that was exposed to 1 μL fd phage at 10^{10} (pfu/mL) for 30 min in "ViriBlock" blocking buffer [39]. The filamentous phage in Fig. 3D is consistent with the size and topography shown in Fig. 3B. Because this silicon slice was dried using nitrogen, the phage showed a compact filamentous structure and lay flat rather than standing up. The phage body stands up or is suspended away from the silicon surface in a liquid environment.

The shape of the target is closely related to the binding location or

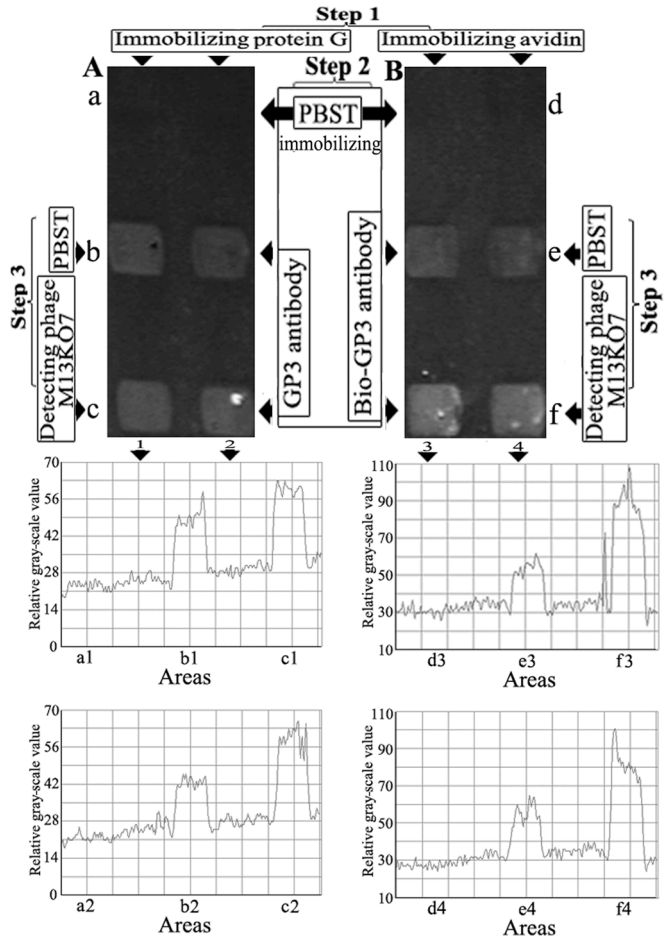

Fig. 2. Phage M13KO7 detection using two kinds of anti-GP3 oriented immobilization. (A) Phage M13KO7 detection using protein G as a ligand. Protein G was first immobilized on two lines, and then anti-GP3 was immobilized as four cells in the bottom two rows. Two cells in the bottom row were used to detect the phage M13KO7 sample. (B) Phage M13KO7 detection using avidin as a ligand. The avidin was first immobilized on two lines, and then anti-GP3 was immobilized as four cells in the bottom two rows. Two cells in the bottom row were used to detect the phage M13KO7 sample.

the grab point on the target. Factors such as shape, weight, volume, etc. of the target are important in influencing the capture efficiency. Targets have different shapes, such as sphere, filament, stick, stellate, and sheet. Different shapes have different suitable capturing positions. When the targeting position is not appropriate, more force is needed to capture the target. Binding spots or positions on the target affect capture efficiency. A long filamentous phage should float in liquid, resembling hair silk, if one end (proximal or distal end) is fixed. The floating and standing posture of the long filament might be subject to greater shear forces than if lying flat. It is difficult to adhere one end of a hair to immobilize it on the surface, while the whole body of hair sticking firmly on the surface is difficult to wash off using water. On the other hand, phage M13KO7 has a greater volume and weight compared to that of the antibody molecule, which needs a stronger binding force and appropriate capturing positions.

3.4. Analysis of the relevant linkage between substrate, ligand, and target

From the substrate to the target, there were several major layers: the substrate, aldehyde group modification, ligand/antibody, and target/M13KO7 layers (Scheme 1). In oriented immobilization, an oriented molecule layer such as protein A, protein G, or avidin was present between the aldehyde group modification and the ligand/antibody layer. Anti-GP3, anti-GP8, protein G, and avidin could be covalently immobilized on the modified substrate due to the covalent bond (Scheme 1①③) based on the reaction of Schiff base between $-NH_4$ and –CHO. The bond coming from the interaction between the antibody and antigen (Scheme 1②⑤) and the bond coming from the interaction between the Fc-anibody and oriented molecule (Scheme 1④) were non-covalent. Force magnitudes were ① ③> ② ④ ⑤.

3.5. Analysis of phage M13KO7 detection

The filamentous structure and possible postures of phage M13KO7 immobilization are shown in Scheme 2. The body of the phage particle was composed of the major coat protein GP8 (about 2800 copies). Three copies of GP3 and two copies of GP6 at the proximal end and three copies of GP7 and two copies of GP9 at the distal end covered the phage particle [40]. There were different antibodies against different proteins of the phage M13KO7. Schemes 2A and E show the direct immobilization of anti-GP3 and anti-GP8 to capture the phage, respectively. Phage M13KO7 was captured horizontally or buried inside anti-GP8 on the surface (Scheme 2E) because anti-GP8 interacted with the protein GP8 on the body of the phage filament. The phages were captured vertically on the surface because anti-GP3 interacted with the protein GP3 on the proximal end of the phage filament (Scheme 2A, B, and C). The direct immobilization of the antibody was random. Owing to steric hindrance and random orientation of the antibodies on the solid–phase surface, the binding activity of the antibody immobilized directly on this surface was usually less than that of the soluble antibody [7, 28]. Some antibodies on the surface could capture the phage M13KO7, while others could not capture (Scheme 2A). This phenomenon was more evident when there were few interacting points on the target, such as anti-GP3. To overcome this problem, protein G was used to modify the silicon surface for oriented immobilization of the antibody. Protein G can specifically bind to the Fc region of various mammalian immunoglobulins [9], while leaving the Fab regions available for antigen binding (Scheme 2B). Because the affinity between protein A or G and the antibody is similar to the affinity between the antibody and antigen (10^7–10^8 M^{-1}), the bond is easily broken by the greater phage volume and weight compared to those of the antibody molecule (see AFM image in Section 3.3). Therefore, the phage M13KO7 could be captured by the sensing surface of protein G/anti-GP3 with a low detection efficiency. The avidin–biotin oriented antibody immobilization model was employed as well (Scheme 2C). An avidin molecule has four biotin-binding sites and hence could capture several antibodies (Scheme 2F). Consequently, an avidin molecule could possibly capture three GP3 proteins simultaneously on the proximal end of one phage M13KO7 filament head proteins through three sites (Scheme 2D). Therefore, the model exhibited a high detection efficiency.

Different numbers of bonds produce different forces. Antibody and antigen could specifically interact with affinity (approximately 10^7–10^8 M^{-1}). In fact, the interaction force of an antibody-antigen pair is approximately 342 pN [15]. As shown in Scheme 2, the phage M13KO7 had three GP3 proteins at the proximal end. Anti-GP3 and protein GP3 interacted one-to-one; three antibodies on the substrate interacted with three GP3 proteins of one phage M13KO7, and the force was approximately 3 × 342 pN. Considering steric hindrance, one of the three GP3 proteins interacted with one antibody on the substrate. This should be the case with the highest probability, and the force would be approximately 342 pN. The phage body is composed of the major coat protein GP8 (Scheme 2E). If phage was buried inside the anti-GP8, and all GP8 proteins interacted with the anti-GP8, the force would be approximately 2800 × 342 pN. The more the binding locations, the greater the resulting force. Considering the shape and steric hindrance, the force was so strong that it increased the possibility of capturing big targets.

4. Conclusions

In conclusion, we developed a label-free and multiplex BIE method to

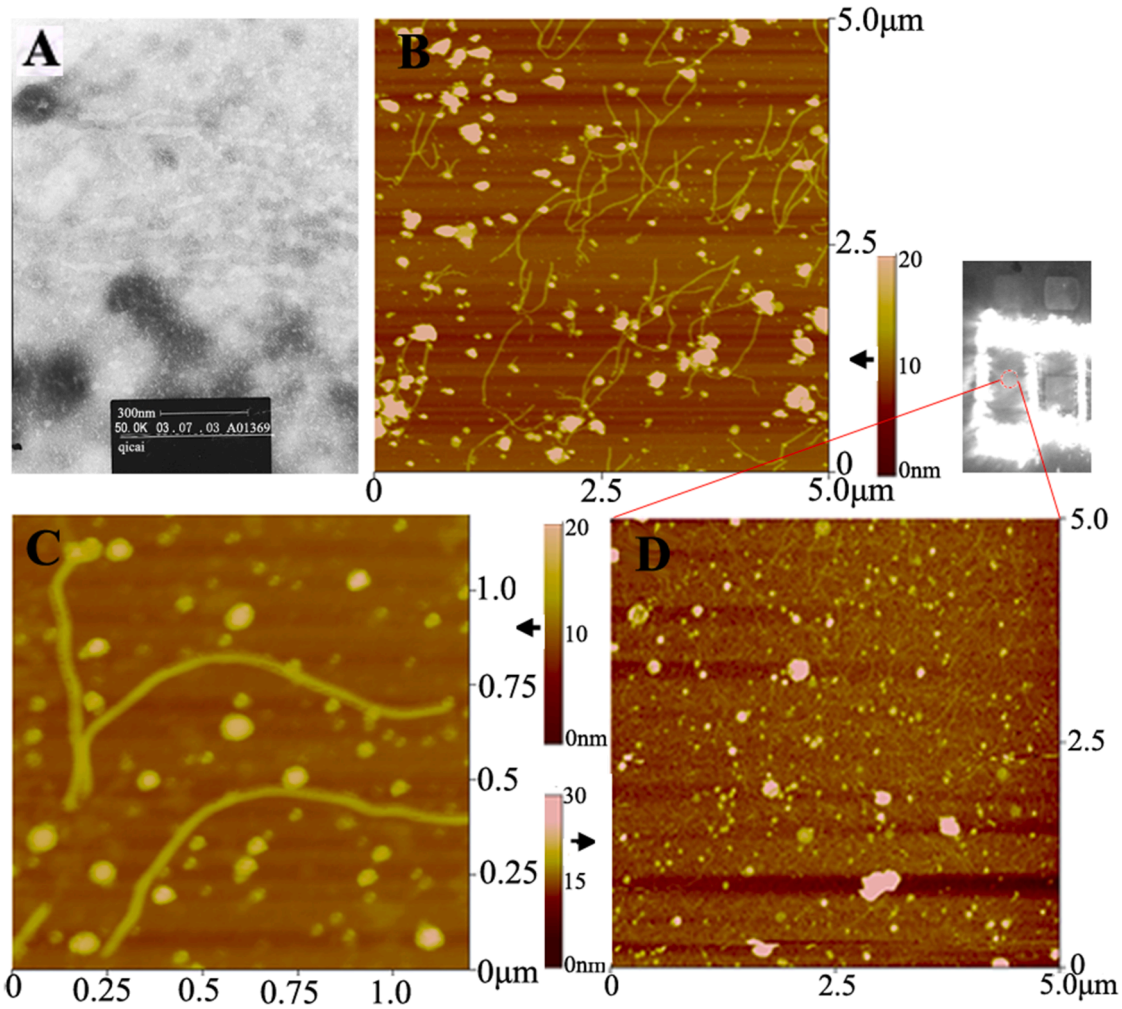

Fig. 3. Microscopic image of phage M13KO7. (A) TEM image of phage M13KO7 in liquid culture medium according to the scan model accelerating voltage 50.0 kV and range 300 nm. (B) AFM height images in tapping mode of phage M13KO7 on the mica surface in (5.0 × 5.0 μm) [19]. (C) AFM height images of phage M13KO7 on the mica surface in (1.0 × 1.0 μm) The whole image was scanned under 5 μm and 0.8846 Hz, and the top left image was scanned under 1.2 μm and 1.209 Hz [19]. (D) The corresponding cells were marked with a marker pen before AFM observation. AFM image of scanning under 5 μm and 1.327 Hz for phage M13KO7 on the sensing surface formed by antibody [19].

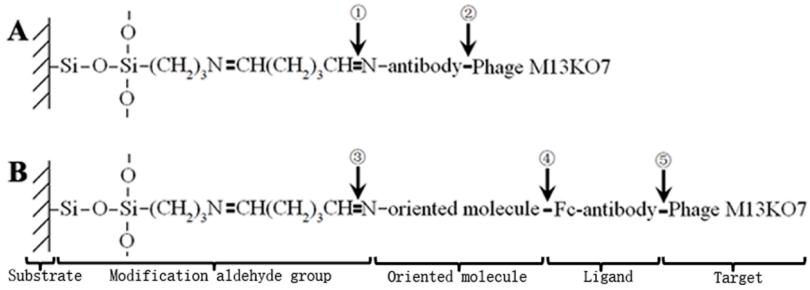

Scheme 1. Schematic illustration of bonds in ligand immobilization and target detection. (A) Direct immobilization. (B) Oriented immobilization. ①③: Bond based on the reaction of schiff base between −CHO of glutaraldehyde and $-NH_4$ of biomolecule. ②⑤: Bond based on the interaction between antibody and antigen. ④: Bond based on specific binding to the Fc portion of immunoglobulin.

detect the phage M13KO7 directly using anti-GP8 as the ligand without oriented immobilization. For big target detection, the capturing binding locations on the target body were significant in enhancing detection efficiency and sensitivity. The surface or edge of the big target falling on the substrate can acquire more binding locations upon interaction with the ligand on a chip rather than the head or angle. Our results suggest that oriented immobilization of antibodies and optimization of binding locations can provide an opportunity to capture big targets when applied in the fields of biosensor detection, micro-particle biological analysis, as well as for *in vitro* diagnosis.

CRediT authorship contribution statement

Cai Qi: Conceptualization, Investigation, Formal and data analysis, Writing – original draft, Writing–review & editing, Methodology, Validation. **Yanxu Zhang**: Investigation, Writing–review, Formal and data

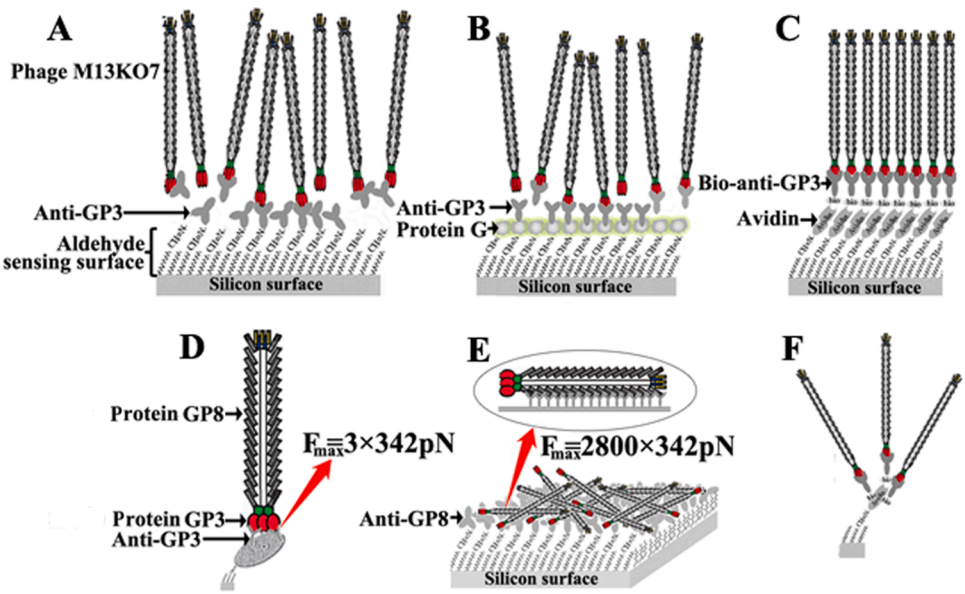

Scheme 2. Schematic illustration of the phage M13KO7 detection. (A) Detection of the phage using direct immobilization of anti-GP3. (B) Detection of the phage using oriented immobilization of protein G; this approach did not have sufficient force to capture the phage. (C) Detection of the phage using the oriented immobilization of avidin–biotin. (D) Schematic illustration of a bacteriophage M13 filament and force analysis of (A, B) and (C, E). (E) Detection of the phage using direct immobilization of anti-GP8. (F) One avidin with four biotin–binding sites can easily capture one phage with three bio-anti-GP3 for acquiring maximum force.

analysis. **Wenjing Lei**: Formal and image analysis, Writing–editing. **Gang Jin**: Conceptualization, Supervision, Writing–review & editing, Resources, Project administration, Funding acquisition.

Declaration of Competing interest

The authors declare that they have no known competing financial interests or personal relationships that could have appeared to influence the work reported in this paper.

Data Availability

No data was used for the research described in the article.

Acknowledgments

This work was surpported by the Fund for Yellow River scholars of Henan University, Guiyang Talent Innovation and Entrepreneur Fundation of China ([2020]-19-12-1), Guizhou Province and Guiyang Science and Technology Planning Project ([2020]4Y188 and [2021]S105) for their supports.

References

[1] R. Ungai-Salánki, B. Csippa, T. Gerecsei, B. Péter, R. Horvath, B. Szabó, Nanonewton scale adhesion force measurements on biotinylated microbeads with a robotic micropipette, J. Colloid Interface Sci. 602 (2021) 291–299, https://doi.org/10.1016/j.jcis.2021.05.180.
[2] J. Smejkal, P. Malý, M. Kuchař, N. Panova, A. Semerádtová, P. Aubrecht, M. Štofik, J. Malý, Cell immunocapture microfluidic chip based on high-affinity recombinant protein binders, Biosens. Bioelectron. 172 (2021), 112784, https://doi.org/10.1016/j.bios.2020.112784.
[3] M. Lijima, T. Nakayama, S. Kuroda, Two-dimensional membrane scaffold for the oriented immobilization of biosensing molecules, Biosens. Bioelectron. 150 (2020), 111860, https://doi.org/10.1016/j.bios.2019.111860.
[4] M. Yoshioka, Y. Mukai, T. Matsui, A. Udagawa, H. Funakubo, Immobilization of ultra-thin layer of monoclonal antibody on glass surface, J. Chromatogr. 566 (1991) 361–368, https://doi.org/10.1016/0378–4347(91)80252–8.
[5] L.C. Shriver-Lake, B. Donner, R. Edelstein, K. Breslin, S.K. Bhatia, F.S. Ligler, Antibody immobilization using heterobifunctional crosslinkers, Biosens. Bioelectron. 12 (1997) 1101–1106, https://doi.org/10.1016/S0956–5663(97)00070–5.
[6] Z.H. Wang, G. Jin, Covalent immobilization of proteins for the biosensor based on imaging ellipsometry, J. Immunol. Methods 285 (2004) 237–243, https://doi.org/10.1016/j.jim.2003.12.002.
[7] Z.H. Wang, G. Jin, Feasibility of protein A for the oriented immobilization of immunoglobulin on silicon surface for a biosensor with imaging ellipsometry, J. Biochem. Biophys. Methods 57 (2003) 203–211, https://doi.org/10.1016/S0165–022X(03)00109–X.
[8] H. Oshima, S. Re, Y. Sugita, Prediction of protein–ligand binding pose and affinity using the gREST+FEP method, J. Chem. Inf. Model. 60 (2020) 5382–5394, https://doi.org/10.1021/acs.jcim.0c00338.
[9] C. Schulte, V. Khayenko, N.F. Nordblom, F. Tippel, V. Peck, A.J. Gupta, H. M. Maric, High–throughput determination of protein affinities using unmodified peptide libraries in nanomolar scale, iScience 24 (2020), 101898, https://doi.org/10.1016/j.isci.2020.101898.
[10] J.A.C. Stein, A. Ianeselli, D. Braun, Kinetic microscale thermophoresis for simultaneous measurement of binding affinity and kinetics, Angew Chem. Int. Ed. Engl. 60 (2021) 13988–13995, https://doi.org/10.1002/anie.202101261.
[11] L.H. Zhang, J. Chen, M.Y. He, X. Su, Molecular dynamics simulation–guided toehold mediated strand displacement probe for single–nucleotide variants detection, Exploration 2 (2021), e20210265, https://doi.org/10.1002/EXP.20210265.
[12] H. Kim, M. Hoshi, M. Iijima, S. Kuroda, C. Nakamura, Development of a universal method for the measurement of binding affinities of antibody drugs towards a living cell based on AFM force spectroscopy, Anal. Methods 12 (2020) 2922–2927, https://doi.org/10.1039/D0AY00788A.
[13] D.E. Leckband, T.L. Kuhl, H.K. Wang, W. Müller, J. Herron, H. Ringsdorf, Force probe measurements of antibody–antigen interactions, Methods 20 (2000) 329–340, https://doi.org/10.1006/meth.1999.0926.
[14] C.H. Wang, R. Hu, J.J. Morrissey, E.D. Kharasch, S. Singamaneni, Single molecule force spectroscopy to compare natural versus artificial antibody–antigen interaction, Small 13 (2017) 1–7, https://doi.org/10.1002/smll.201604255.
[15] B. Gao, G. Jin, Investigation of interaction force between surface immobilized ligand and objective molecule using shear flow chamber, Prog. Biochem. Biophys. 32 (2005) 982–990. https://europepmc.org/article/cba/598693.
[16] J.C. Liu, D. Zhang, D.Q. Yu, M.X. Ren, J.J. Xu, Machine learning powered ellipsometry, Light Sci. Appl. 10 (2021) 55–62, https://doi.org/10.1038/s41377–021–00482–0.
[17] Y.M. Bae, K.W. Park, B.K. Oh, W.H. Lee, J.W. Choi, Immunosensor for detection of salmonella typhimurium based on imaging ellipsometry, Colloids Surf. A Physicochem. Eng. Asp. 257–258 (2005) 19–23, https://doi.org/10.1016/j.colsurfa.2004.10.082.
[18] C. Qi, X.S. Tian, S. Chen, J.H. Yan, Z. Cao, K.G. Tian, G.F. Gao, G. Jin, Detection of avian influenza virus subtype H5 using a biosensor based on imaging ellipsometry, Biosens. Bioelectron. 25 (2010) 1530–1534, https://doi.org/10.1016/j.bios.2009.10.030.
[19] C. Qi, Y. Lin, J. Feng, Z.H. Wang, C.F. Zhu, Y.H. Meng, X.Y. Yan, L.J. Wan, G. Jin, Phage M13KO7 detection with biosensor based on imaging ellipsometry and AFM microscopic confirmation, Virus Res. 140 (2009) 79–84, https://doi.org/10.1016/j.virusres.2008.11.010.
[20] C. Qi, H. Zhang, L. Liu, R.K. Yang, T.F. Kang, W.X. Hao, G. Jin, T.J. Jiang, Analysis of interactions between SNARE proteins using imaging ellipsometer coupled with microfluidic array, Sci. Rep. 4 (2014) 5341–5346, https://doi.org/10.1038/srep05341.
[21] W. Wang, C. Qi, T.F. Kang, Y. Niu, G. Jin, Y. Chen, Y.Q. Ge, Analysis of interaction between tropomyosin allergen and antibody using a biosensor based on imaging ellipsometry, Anal. Chem. 85 (2013) 4446–4452, https://doi.org/10.1021/ac303783j.
[22] Z.H. Wang, G. Jin, Visualization of the interaction between IL-6 and IL-6R by imaging ellipsometry, Chin. J. Biotechnol. 18 (2002) 99–101. https://europepmc.org/article/med/11977610.

[23] Y. Niu, T.F Kang, G. Jin, Joint detection of tumor markers with imaging ellipsometry biosensor, Thin Solid Films 571 (2014) 453–462, https://doi.org/10.1016/j.tsf.2014.01.043.
[24] C. Qi, W. Zhu, Y. Niu, H.G. Zhang, G.Y. Zhu, Y.H. Meng, S. Chen, G. Jin, Detection of hepatitis B markers using biosensor based on imaging ellipsometry, J. Viral Hepat. 16 (2009) 822–832, https://doi.org/10.1111/j.1365−2893.2009.01123.x.
[25] Z.L. Wang, X.Y. Yunlei, W. Liu, Y.K. Li, Z.X. Cai, X. Fu, G. Jin, Y. Niu, C. Qi, Y. P. Chen, Nanoparticles−enabled surface−enhanced imaging ellipsometry for amplified biosensing, Anal. Chem. 91 (2019) 6769–6774, https://doi.org/10.1021/acs.analchem.9b00846.
[26] Y.K. Li, Y. Zhang, X. Yan, G. Jin, Label-free sandwich imaging ellipsometry immunosensor for serological detection of procalcitonin, Anal. Chem. 90 (2008) 8002–8010, https://doi.org/10.1021/acs.analchem.8b00888.
[27] P. Van Wezenbeek, J.G. Schoenmakers, Nucleotide sequence of the genes III, VI and I of bacteriophage M13, Nucleic Acids Res. 6 (1979) 2799–2818, https://doi.org/10.1093/nar/6.8.2799.
[28] S. Kanno, Y. Yanagida, T. Haruyama, E. Kobatake, M. Aizawa, Assembling of engineered IgG−binding protein on gold surface for highly oriented antibody immobilization, J. Biotechnol. 76 (2000) 207–214, https://doi.org/10.1016/S0168−1656(99)00186−8.
[29] H. Arwin, S. Welinklinstorm, R. Jansson, Off−null ellipsometry revisited: basic considerations for measuring surface concentrations at solid/liquid interfaces, J. Colloid Interface Sci. 156 (1993) 377–382, https://doi.org/10.1006/jcis.1993.1125.
[30] G. Jin, R. Jansson, H. Arwin, Imaging ellipsometry revisited: developments for visualization of thin transparent layers on silicon substrates, Rev. Sci. Instrum. 67 (1996) 2930–2936, https://doi.org/10.1063/1.1147074.
[31] G. Jin, P. Tengvall, I. Lundstrom, H. Arwin, A biosensor concept based on imaging ellipsometry for visualization of biomolecular interactions, Anal. Biochem. 232 (1995) 69–72, https://doi.org/10.1006/abio.1995.9959.
[32] M. Stenberg, H. Nygren, The use of the isoscope ellipsometer in the study of adsorbed proteins and biospecific binding reactions, J. Physique 44 (1983) 83–86, https://doi.org/10.1051/jphyscol:19831017.
[33] Y.S. Lo, Y.J. Zhu, T.P. Beebe, Loading−rate dependence of individual ligand−receptor bond−rupture forces studied by atomic force microscopy, Langmuir 17 (2001) 3741–3748, https://doi.org/10.1021/la001569g.
[34] P.Q. Ying, G. Jin, Z. Tao, Competitive adsorption of collagen and bovine serum albumin−Effect of the surface wettability, Colloid Surface B 33 (2004) 259–263, https://doi.org/10.1016/j.colsurfb.2003.10.015.
[35] P.K. Ngai, F. Ackermann, H. Wendt, R. Savoca, H.R. Bosshard, Protein A antibody−capture ELISA(pace) : an ELISA format to avoid denaturation of surface−adsorbed antigens, J. Immunol. Methods 158 (1993) 267–276, https://doi.org/10.1016/0022−1759(93)90223−T.
[36] E. Zacco, M.I. Pividori, S. Alegret, Electrochemical biosensing based on universal affinity biocomposite platforms, Biosens. Bioelectron. 21 (2006) 1291–1301, https://doi.org/10.1016/j.bios.2005.05.016.
[37] L. Viveros, S. Paliwal, D. McCrae, J. Wild, A. Simonian, A fluorescence−based biosensor for the detection of organophosphate pesticides and chemical warfare agents, Sensors Actuators B-Chem 115 (2006) 150–157, https://doi.org/10.1016/j.snb.2005.08.032.
[38] X. Ji, J. Oh, A.K. Dunker, K.W. Hipps, Effects of relative humidity and applied force on atomic force microscopy images of the flamentous phage fd, Ultramicroscopy 72 (1998) 165–176, https://doi.org/10.1016/S0304−3991(97)00169−1.
[39] S.R. Nettikadan, J.C. Johnson, C. Mosher, E. Henderson, Virus particle detection by solid phase immunocapture and atomic force microscopy, Biochem. Biophys. Res. Commun. 311 (2003) 540–545, https://doi.org/10.1016/j.bbrc.2003.10.022.
[40] D. Stopar, R.B. Spruijt, C.J. Wolfs, M.A. Hemminga, Protein−lipid interactions of bacteriophage M13 major coat protein, Biochimi. Biophys. Acta. 1611 (2003) 5–15, https://doi.org/10.1016/S0005−2736(03)00047−6.